Heteromultimeric Delayed-Rectifier K$^+$ Channels in Schwann Cells: Developmental Expression and Role in Cell Proliferation

Alexander Sobko,[1] Asher Peretz,[1] Orian Shirihai,[2] Sarah Etkin,[1] Vera Cherepanova,[1] Daniel Dagan,[2] and Bernard Attali[1]

[1]*Neurobiology Department, Weizmann Institute of Science, Rehovot 76100, Israel, and* [2]*Bruce Rappaport Faculty of Medicine, Bernard Katz Minerva Center for Cell Biophysics, Technion, Haifa 31096, Israel*

Schwann cells (SCs) are responsible for myelination of nerve fibers in the peripheral nervous system. Voltage-dependent K$^+$ currents, including inactivating A-type (K_A), delayed-rectifier (K_D), and inward-rectifier (K_{IR}) K$^+$ channels, constitute the main conductances found in SCs. Physiological studies have shown that K_D channels may play an important role in SC proliferation and that they are downregulated in the soma as proliferation ceases and myelination proceeds. Recent studies have begun to address the molecular identity of K$^+$ channels in SCs. Here, we show that a large repertoire of K$^+$ channel α subunits of the *Shaker* (Kv1.1, Kv1.2, Kv1.4, and Kv1.5), *Shab* (Kv2.1), and *Shaw* (Kv3.1b and Kv3.2) families is expressed in mouse SCs and sciatic nerve. We characterized heteromultimeric channel complexes that consist of either Kv1.5 and Kv1.2 or Kv1.5 and Kv1.4. In postnatal day 4 (P4) sciatic nerve, most of the Kv1.2 channel subunits are involved in heteromultimeric association with Kv1.5. Despite the presence of Kv1.1 and Kv1.2 α subunits, the K$^+$ currents were unaffected by dendrotoxin I (DTX), suggesting that DTX-sensitive channel complexes do not account substantially for SC K_D currents. SC proliferation was found to be potently blocked by quinidine or 4-aminopyridine but not by DTX. Consistent with previous physiological studies, our data show that there is a marked downregulation of all K_D channel α subunits from P1–P4 to P40 in the sciatic nerve. Our results suggest that K_D currents are accounted for by a complex combinatorial activity of distinct K$^+$ channel complexes and confirm that K_D channels are involved in SC proliferation.

Key words: K$^+$ channels; Schwann cells; myelination; proliferation; development; ion channels; heteromultimeric association

Schwann cells (SCs) are responsible for myelinating axons of the peripheral nervous system, a phenomenon that is crucial for the maintenance of saltatory conduction of nerve impulses. In the Schwann cell lineage, multipotent neural crest cells give rise to SC precursors, which in turn give rise to SCs (for review, see Mirsky and Jessen, 1996; Zorick and Lemke, 1996). After a period of migration and vigorous proliferation, the cells interact with nerve bundles, and those associating with large axons stop dividing and myelinate, whereas those associated with smaller axons subsequently mature as nonmyelin-forming SCs. If the nerve is injured via mechanical trauma or demyelinating diseases, SCs can reenter the mitotic cycle to restore the integrity of the myelin sheath and contribute to functional recovery of the nerve fibers. SCs and neurons exert powerful influences on each other, during both early development and differentiation, as well as in the course of peripheral nerve regeneration. Myelinating SCs initiate the process of myelination in response to contact-mediated axonal signals (Mirsky and Jessen, 1996; Zorick and Lemke, 1996). SCs also provide important support for axons, strongly influencing the organization of ionic channels along axonal membranes (Rasband et al., 1998).

Voltage-dependent K$^+$ channels (Kv channels) constitute the major ionic conductance detected in SCs (Barres et al., 1990; Chiu, 1991; Ritchie, 1992; Sontheimer, 1994). These include inactivating A-type (K_A), delayed-rectifier (K_D), and inward-rectifier (K_{IR}) K$^+$ channels (Chiu et al., 1984; Shrager et al., 1985; Konishi, 1989; Wilson and Chiu, 1990a,b; Amedee et al., 1991; Verkhartsky et al., 1991a,b; Baker and Ritchie, 1993). However, the functions of these K$^+$ channel subsets are still not clear. It has been suggested that SC K_{IR} channels play a role in buffering activity-dependent K$^+$ accumulation during early myelinogenesis and in adult nerves (Konishi, 1990; Wilson and Chiu, 1990a,b). K_D channels have been implicated in SC proliferation during development and after Wallerian degeneration of sciatic nerves (Chiu and Wilson, 1989; Konishi, 1989; Wilson and Chiu, 1990a). Interestingly, physiological studies have revealed that K_D and K_{IR} channels are downregulated in the soma as myelination proceeds and proliferation ceases (Konishi, 1990; Wilson and Chiu, 1990a). However, developmental studies at the protein level are not documented.

Recent studies have begun to address the molecular identity of K$^+$ channels in SCs. The *Shaker*-like delayed-rectifier Kv1.1, Kv1.2, and Kv1.5 and the inward-rectifier IRK1 and IRK3 α subunits were shown to be expressed in SCs of the rat sciatic nerve (Chiu et al., 1994; Mi et al., 1995, 1996; Rasband et al., 1998). We recently found that Kv2.1 and Kv3.1b delayed-rectifier α subunits are abundantly expressed in mouse SCs and sciatic nerve (Sobko et al., 1998). Thus, the K_D currents are probably accounted for by the activity of different K$^+$ channel complexes. However, it is not known whether these channel complexes assemble as homomultimers or heteromultimers *in vivo*.

The goals of this study were (1) to identify at the mRNA and protein levels the K$^+$ channel α subunits underlying the K_D currents in mouse SCs and to determine whether they could assemble as heteromultimeric complexes, (2) to analyze the developmental profile of the various α subunits in the sciatic nerve, and (3) to compare the ability of K$^+$ channel blockers to depress the SC K$^+$ currents with their capacity to inhibit SC proliferation. Our results indicate that a complex repertoire of Kv channel α subunits is expressed in cultured SCs and sciatic nerve. We found heteromultimeric association between Kv1.5 and either Kv1.2 or Kv1.4. A marked downregulation of all delayed-rectifier K$^+$ channel α subunits was detected in the sciatic nerve from postnatal day 1 (P1)–P4 to P40. Our findings suggest further that K_D channels are important for SC proliferation.

MATERIALS AND METHODS

Materials. Quinine, quinidine, 4-aminopyridine (4-AP), tetraethylammonium (TEA), and protein A/G Sepharose were purchased from Sigma (St. Louis, MO). Charybdotoxin (CTX), dendrotoxin I (DTX), and Agitoxin-2 (AgTx) were kindly provided by Alomone Labs (Jerusalem, Israel). The source of antibodies was as follows: monoclonal and polyclonal antibodies to Kv1.1, Kv1.2, Kv1.4, Kv1.5, and Kv2.1 were from Upstate Biotechnology (Lake Placid, NY); anti-Kv1.1, anti-Kv1.2, Kv1.4, Kv1.5, anti-Kv3.1b, and anti-Kv3.2 polyclonal antibodies were purchased from Alomone Labs (Jerusalem, Israel); and rabbit anti-S-100 was from Sigma. Goat anti-mouse, goat anti-rabbit fluorescein (FITC)- or rhodamine (TRITC)-conjugated and horseradish peroxidase (HRP)-conjugated secondary antibodies were from Jackson ImmunoResearch (West Grove, PA). [^{3}H]Thymidine (29 Ci/mmol) was purchased from Amersham (Arlington Heights, IL).

Schwann cell cultures, proliferation, and immunocytochemistry. Primary SC cultures were prepared from P4 mouse sciatic nerves according to Brockes et al. (1979). Cells were plated on poly-D-lysine-coated Petri dishes or glass coverslips and grown in DMEM–F-12 supplemented with 2 mM glutamine, 10% fetal calf serum (FCS), and antibiotics. Under these conditions, which allowed proliferation and inhibited the expression of the myelin phenotype, we obtained 90–95% pure Schwann cell cultures, as controlled by S-100 immunofluorescence. [^{3}H]Thymidine incorporation (0.2 μCi/well) was assayed in SCs cultured as indicated, in serum-containing medium, in serum-deprived medium (DMEM–F-12), or in serum-free defined medium supplemented with either 5 μg/ml insulin, 5 μg/ml transferrin and 5 ng/ml sodium selenite (SATO1), or with SATO1 containing 5 ng/ml PDGF and 5 ng/ml basic FGF (bFGF) (SATO2). Cells were treated with various concentrations of channel blockers as indicated, and the assay was performed as described previously (Attali et al., 1997). Immunocytochemistry was performed (Attali et al., 1997; Sobko et al., 1998), and cells were viewed using a Zeiss (Oberkochen, Germany) Axioplan microscope equipped with phase-contrast and epifluorescent optics.

Preparation of cell lysates and membrane solubilization. Confluent cell cultures (60 or 100 mm dishes) were washed twice with cold PBS and scraped on ice in PBS containing 1 mM PMSF. After centrifugation, cell pellets or acutely isolated sciatic nerves were either frozen in liquid nitrogen and kept at -80°C until use or homogenized in the buffer containing 50 mM Tris, pH 7.4, 1 mM EDTA, 1 mM PMSF, 10 μg/ml aprotinin, and 10 μg/ml leupeptin and centrifuged at $21,000 \times g$ for 30 min at 4°C. The pellet (crude membranal fraction) was sonicated and resuspended in either SDS-sample buffer (Laemmli, 1970) for direct immunoblot analysis or in the solubilization buffer (glycerol 10%, 50 mM HEPES, pH 7.4, 10 mM EDTA, NaCl 150 mM, 1.5 mM MgCl$_2$, 1% Triton X-100, 1 mM PMSF, 10 μg/ml aprotinin, and 10 μg/ml leupeptin) for immunoprecipitation. Protein concentration was determined using Bio-Rad (Hercules, CA) protein assay solution with bovine serum albumin and human immunoglobulin as a standard.

Immunoprecipitation. Samples were incubated with shaking in the solubilization buffer for 1 hr at 4°C and spun at $21,000 \times g$. Using identical amounts of input proteins for the various treatments, the extracts (supernatants) were precleared with 1:1 slurry of protein A/G Sepharose (30 μl/ml of extract) and equilibrated in lysis buffer for 1 hr at 4°C with shaking. After a short spin, the supernatant was transferred into a new tube and incubated with the antibodies or the respective preimmune serum at 4°C for 4 hr or overnight with shaking. Immune com-

plexes were pooled-down after the addition of 30 μl of protein A/G Sepharose for 1 hr at 4°C with shaking. Where indicated, the supernatant was transferred into a new tube and was reused in a second round of immunoprecipitation. Immunoprecipitates were washed three times in the solubilization buffer, and beads were finally resuspended in 30 μl of 2$\times$ SDS-sample buffer and boiled at 100°C for 5 min to elute the precipitated proteins. The eluent was electrophoresed on SDS-PAGE with standard molecular weight markers.

Immunoblot analysis. After separation on SDS-PAGE, proteins were electrotransferred to nitrocellulose blots. Blots were blocked in PBS containing 10% nonfat milk and 0.05% Tween 20 (Western buffer) for 1 hr at room temperature with shaking. Then, blots were incubated with the respective antibody overnight at 4°C or for 4 hr at room temperature. After three washes with Western buffer, blots were incubated for 1 hr with HRP-conjugated secondary antibody, followed by extensive washes in PBS. Labeled proteins were detected by enhanced chemiluminescence (ECL) (Amersham). Band signals corresponding to immunoreactive proteins were measured and scanned by image densitometry using NIH Image 1.54 and Adobe Photoshop 3.0 software. Densitometric data were normalized to respective protein input assessed by Ponceau staining of blots. In addition to tests performed previously in transfected HEK 293 cells (Attali et al., 1997), we checked directly for antibody specificity in SC extracts by preadsorbing the anti-Kv channel antibodies with their respective antigens for 1 hr at room temperature as follows (see Fig. 3*B*): anti-Kv1.1, anti-Kv1.2, and anti-Kv1.5 antibodies (Upstate Biotechnology and Alomone Labs) were preadsorbed with the respective glutathione *S*-transferase (GST) channel fusion proteins (3 mg/mg antibody; Alomone Labs) spanning similar or overlapping C-terminus domains of the immunizing antigens (residues 416–495, 417–498, and 513–602 of mouse Kv1.1, rat Kv1.2, and mouse Kv1.5, respectively). Because the antigen (residues 13–37 of rat Kv1.4) of anti-Kv1.4 antibodies from Upstate Biotechnology was not available to us, we also used anti-Kv1.4 antibodies from Alomone Labs (residues 589–655 of rat Kv1.4) to test for specificity by preadsorbing antibodies with the corresponding GST channel fusion protein (3 mg/mg antibody). The N-terminus-directed (Upstate Biotechnology) and C-terminus-directed (Alomone Labs) anti-Kv1.4 antibodies labeled the same molecular weight immunoreactive protein in SC extracts, further demonstrating the specificity of the anti-Kv1.4 antibodies from both sources. Anti-Kv2.1 (Upstate Biotechnology), anti-Kv3.1b, and anti-Kv3.2 (Alomone labs) antibodies were preadsorbed with their immunizing peptide antigens (1 mg peptide/mg antibody) consisting of residues 837–853, 567–585, and 184–204 of the respective rat channel sequences. In all cases, the labeling was specific and was unaffected by unrelated (BSA, 3 mg/mg antibody) or irrespective antigens.

Molecular cloning and semiquantitative PCR. Molecular cloning of Kv channel α subunits was performed by screening a rat Schwann cell cDNA library (kindly provided by Dr. G. Lemke, Salk Institute, La Jolla) at low stringency using the S5-S6 region of Kv1.1 as an hybridizing probe (Attali et al., 1993). We also performed a reverse transcription-PCR (RT-PCR) cloning using degenerate oligonucleotides as described previously (Attali et al., 1997). The upstream primer (5′ AAYGAGTACTTCTTYG-AYMG 3′) corresponded to a conserved region NEYFFDR, located upstream of the first transmembrane domain S1. The downstream primer (5′ NCCRTANCCNRNNGWNGA 3′) corresponded to the most conserved H5 pore signature sequence TTVGYG.

For semiquantitative RT-PCR, the reverse-transcription was performed as described previously (Attali et al., 1997). Unique primer pairs encoding specific 3′ coding region of the respective Kv channels were used for RT-PCR amplification: Kv1.2 sense 5′ CACCGGGAGACA-GAGGGA 3′ (1249–1266) and Kv1.2 antisense 5′ TCAGACATCAGT-TAACAT 3′ (1479–1497); and Kv1.5 sense 5′ CATCGGGAGACA-GACCAC 3′ (1834–1851) and Kv1.5 antisense 5′TTACAAATCTGT-TTCCCG 3′ (2089–2107). A semiquantitative PCR analysis was performed to quantify the input mRNA and related cDNA of the various samples. The coamplification of an internal control housekeeping S16 mouse ribosomal protein mRNA was performed using an upstream primer (S16 sense, 5′ AGGAGCGATTTGCTGGTG 3′) and a downstream primer (S16 antisense, 5′ CAGGGCCTTTGAGATGGA 3′), which amplified a 102 bp cDNA fragment. Equal aliquots of each PCR reaction were removed and analyzed by 1.2% agarose gel electrophoresis, Southern blotted onto nylon membranes, and probed with an unique internal [^{32}P]-labeled oligonucleotide. Data were quantified by scanning the labeled bands as above, and the optical densities of Kv channel bands were normalized to the S16 signal.

Electrophysiology. Cultured SCs, plated on poly-D-lysine-coated glass coverslips, were placed in a 1 ml recording chamber mounted on the stage of a Zeiss Axiovert 35 inverted microscope. The whole-cell configuration of the patch-clamp technique (Hamill et al., 1981) was used to record the macroscopic whole-cell currents at room temperature (22 ± 1°C). Signals were amplified using an Axopatch 200B patch-clamp amplifier (Axon Instruments), filtered below 2 kHz via a 4-pole Bessel low-pass filter. Data were sampled at 5 kHz and analyzed using pClamp 6.0.2 software (Axon Instruments) and an IBM-compatible 486 computer, with a Digi-Data 1200 interface (Axon Instruments). The patch pipettes were pulled from borosilicate glass (fiber-filled) with resistance of 4–8 MΩ and were filled with (in mM): 120 KCl, 2 MgCl$_2$, 1 CaCl$_2$, 11 EGTA, 10 HEPES, and 11 glucose, pH 7.4. The external solution contained (in mM): 140 NaCl, 5 KCl, 5 CaCl$_2$, 2 MgCl$_2$, 11 glucose, and 10 HEPES, pH 7.4. TEA (10 mM), BaCl (0.5 mM), and the other blockers were externally perfused to block the K$^+$ currents. Series resistances were within 10–16 MΩ and were compensated by 85–90%. Traces were leak-subtracted by the Clampfit program of the pClamp 6.02 software and further analyzed by the Axograph 3.0 software (Axon Instruments). Activation and steady-state inactivation curves were fitted by the Boltzmann distribution (assuming reversal potential of −85 mV, calculated by Nernst equation):

$$I/I_{\max} = a/\{1+\exp[(V_{50} - V_K)/s]\},$$

where V_{50} is the half-maximal activation (for the steady-state activation protocol) or the voltage at which half of the steady-state inactivation was removed, and s is the slope of the curve. The transient and the sustained components of the K$^+$ currents were measured at the peak and the end (400 msec) of the depolarizing traces, respectively. All data were expressed as mean ± SEM. Statistically significant differences were assessed by Student's *t* test.

RESULTS

Schwann cells express K_A and K_D currents: pharmacology and molecular characterization of Kv channel α subunits

SCs were isolated from P4 mouse sciatic nerves and grown *in vitro* for 2–7 d in the presence of serum. Under these conditions, the SCs proliferated actively and expressed the SC marker S-100 (see Fig. 3*A*). Macroscopic currents were recorded from cultured cells using the whole-cell configuration of the patch-clamp technique (Hamill et al., 1981). In agreement with previous studies (Hoppe et al., 1989; Konishi, 1989; Wilson and Chiu, 1990a; Amedee et al., 1991), the mouse SCs exhibited prominent voltage-gated outward K$^+$ currents that activated after membrane depolarization (Fig. 1*A*). Whole-cell recordings revealed the presence of transient K_A and sustained K_D current components (Fig. 1*A*). Both K$^+$ current components were activated above a threshold of approximately −50 mV, which is close to the SC resting potential. Activation curves could be described by single Boltzmann distributions with $V_{50} = -13.7 \pm 0.9$ mV and $V_{50} = -18.1 \pm 0.8$ mV, and slopes $s = -8.1 \pm 0.5$ and $s = -6.5 \pm 0.4$ for the transient and the sustained components, respectively (±SEM; $n = 16$) (Fig. 1*B*, *left*). The steady-state inactivation curves (Fig. 1*B*, *right*) indicated that the transient component inactivated at slightly more hyperpolarized potentials (by −8.1 mV), relative to the sustained component with $V_{50} = -17.7 \pm 1.5$ mV and $V_{50} = -9.6 \pm 0.3$ mV, and slopes $s = 16.5 \pm 0.6$ and $s = 16.5 \pm 0.6$, respectively ($n = 7$).

Figure 2 illustrates the pharmacology of the mouse SC K$^+$ currents. In addition to broad-spectrum K$^+$ channel blockers (TEA, 4-AP, quinine, quinidine, Ba^{2+}, and clofilium), we also used channel toxins, whose spectrum activity is more restricted. For example, the scorpion toxin CTX is known to block Kv channels comprising at least one Kv1.3 α subunit with high affinity, whereas the snake toxin DTX specifically inhibits Kv1.1, Kv1.2, and Kv1.6 homomultimeric channels (MacKinnon, 1991;
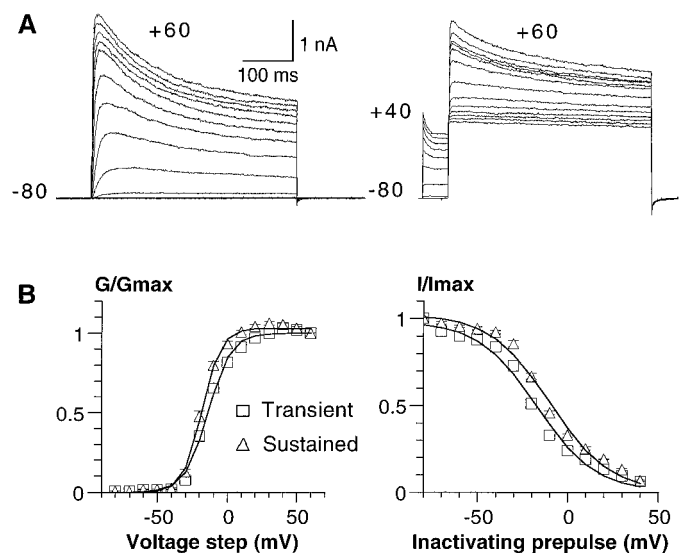

Figure 1. Activation and inactivation characteristics of K$^+$ currents in cultured SCs. *A*, *Left*, In these representative whole-cell recordings, the cells were stepped for 400 msec from a holding potential of −80 to +60 mV in 10 mV increments. *Right*, For the steady-state inactivation protocol, the cell membrane was subjected to inactivating prepulses of 1 sec duration from −70 to +40 mV in 10 mV increments, before the 400 msec test pulse to +60 mV. *B*, *Left*, The normalized conductance was plotted against voltage steps for the transient (*open triangles*) and sustained (*open squares*) components. The curves were fitted using a single Boltzmann distribution with the parameters of $V_{50} = -13.7 \pm 0.9$ mV and $V_{50} = -18.1 \pm 0.8$ mV, and slopes of $s = -8.1 \pm 0.5$ and $s = -6.5 \pm 0.4$ ($n = 16$) for the transient and sustained components, respectively. *Right*, The steady-state inactivation curves of the transient (*open triangles*) and sustained (*open squares*) components gave the parameters of $V_{50} = -17.7 \pm 1.5$ mV and $V_{50} = -9.6 \pm 0.3$ mV, and slopes of $s = 16.5 \pm 0.6$ and $s = 16.5 \pm 0.6$ ($n = 7$), respectively.

Grissmer et al., 1994; Tytgat et al., 1995). Likewise, AgTx displays a very high affinity for Kv1.1, Kv1.2, Kv1.3, and Kv1.6 channels (Garcia et al., 1994). Our results show that the SC K$^+$ currents are sensitive to block by 3 mM 4-AP (76 ± 4%; $n = 12$), 10 mM TEA (65 ± 6%; $n = 11$), and 0.5 mM Ba^{2+} (32 ± 14%; $n = 7$) as measured by a +50 mV test pulse. These K$^+$ channel blockers did not discriminate between K_A and K_D currents. However, 3 mM 4-AP could totally eliminate K_A, leaving an unblocked fraction (~30%) of K_D (Fig. 2*B*). The block of 4-AP and to a lesser extent that of TEA and Ba^{2+} were voltage-dependent, with a maximum block in the voltage range of −20 to 0 mV (Fig. 2*D*, *left*). The 4-AP block decreased with increasing depolarization, suggesting that 4-AP binding occurs preferentially in the closed state (Yeh et al., 1976; Wang et al., 1995). Both K_A and K_D currents were potently blocked by 100 μM quinine (76 ± 9%; $n = 8$), 100 μM quinidine (100%; $n = 8$), and 10 μM clofilium (70 ± 8%; $n = 7$) as measured by a +50 mV test pulse (data not shown). The SC K$^+$ currents were totally insensitive to 100 nM DTX ($n = 6$), 100 nM CTX ($n = 6$), and 10 nM AgTx ($n = 6$) (Fig. 2*D*, *right*).

Next, we characterized extensively the molecular identity of the Kv channel α subunits in cultured SCs and the sciatic nerve. For this purpose, we used RT-PCR cloning, conventional screening of a rat Schwann cell cDNA library, and immunodetection using a battery of subunit-specific polyclonal and monoclonal antibodies. From the Schwann cell cDNA library, we fished out partial and full-length cDNA clones encoding the *Shaker* Kv1.4 and Kv1.5 α subunits, respectively. For RT-PCR cloning, mRNA extracts prepared from cultured mouse SCs (4 d *in vitro*) were
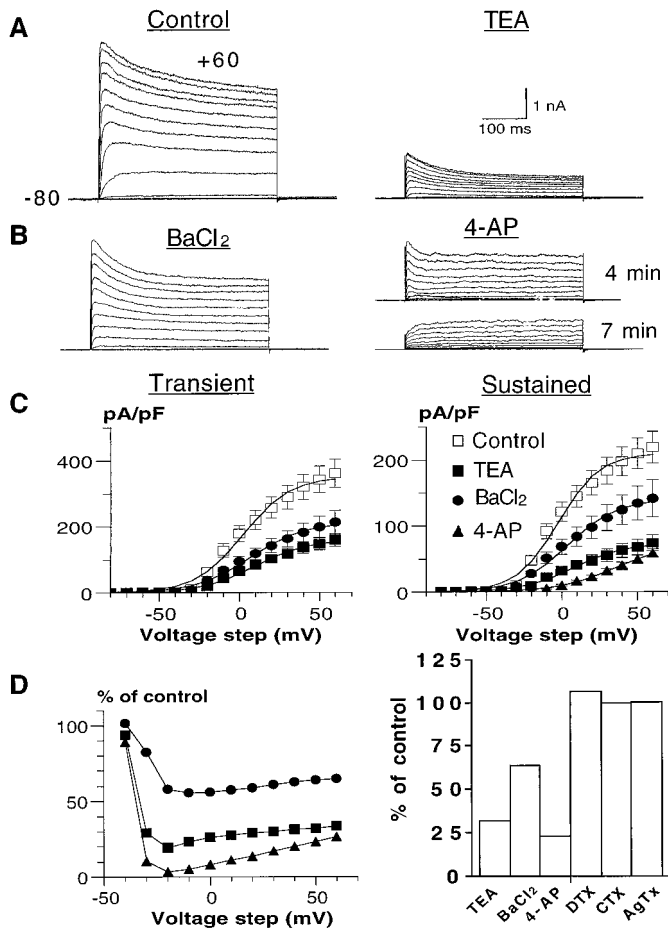
Figure 2. Pharmacology of the SC K$^+$ currents. *A, B,* Current traces of a control cell (*A, left*) and after external application of 10 mM TEA (*A, right*), 0.5 mM BaCl$_2$ (*B, left*), and 3 mM 4-AP (*B, right*). Note that in the 4-AP experiment shown, the transient component totally disappears after 7 min application (*bottom traces*) but remained partially inhibited after 4 min exposure (*top traces*). The activation protocol was the same as in Figure 1. *C,* The current density (pA/pF)/voltage curves of the transient (*left*) and sustained (*right*) components are shown for control cells (*open squares*) and after application of 10 mM TEA (*filled squares*), 0.5 mM BaCl$_2$ (*filled circles*), and 3 mM 4-AP (*filled triangles*). The current density/voltage curve of the transient component in the presence of 4-AP is not shown, because 4-AP totally eliminates this transient current. *D, Left,* Voltage-dependent block of 10 mM TEA, 0.5 mM BaCl$_2$, and 3 mM 4-AP is shown. The percentage of block is plotted versus voltage step. *Right,* Effects of 10 mM TEA (*n* = 11), 0.5 mM BaCl$_2$ (*n* = 7), 3 mM 4-AP (*n* = 12), 100 nM DTX (*n* = 6), 100 nM CTX (*n* = 6), and 10 nM AgTx (*n* = 6) were expressed as percentage of control current elicited by a +50 mV step (400 msec).

Figure 3. Immunodetection of Kv channel α subunits in cultured SCs. *A,* Cultured cells were subjected to immunofluorescence analysis with anti-S-100 antibody to confirm SC identity. Indirect immunofluorescence with anti-rabbit FITC was used for detection. Scale bar, 20 μM. *B,* Immunoblot analysis of Schwann cell cultures with antibodies to Kv channel α subunits. Membrane fractions of mouse primary cultured SCs were subjected to immunoblot analysis with subunit-specific antibodies to Kv1.1, Kv1.2, Kv1.4, Kv1.5, Kv2.1, Kv3.1b, and Kv3.2 α subunits. To check the specificity of antibody labeling toward SC membrane extracts, each antiserum was preincubated for 1 hr at room temperature in the presence (+) or absence (-) of its respective antigen, as indicated in Materials and Methods. HRP-conjugated secondary antibodies and ECL were used for detection.

subjected to RT-PCR using degenerate oligonucleotides encoding conserved domains of *Shaker, Shab, Shaw,* and *Shal* family members (see Materials and Methods; Attali et al., 1997). The upstream primer corresponded to a conserved region NEYFFDR, located upstream of the first transmembrane domain S1. The downstream primer encoded the most conserved H5 pore signature sequence TTVGYG. After this strategy, Kv1.1, Kv1.2, Kv1.5, Kv1.6, Kv2.1, Kv2.2, Kv3.1, and Kv3.2 channel α subunits were identified. To confirm the cloning data and to characterize at the protein level the various Kv channel α subunits, we performed immunoprecipitation, immunoblot, and immunofluorescence analyses using various monoclonal and polyclonal antibodies (Figs. 3–7). The specificity of antibody staining in SCs was di-
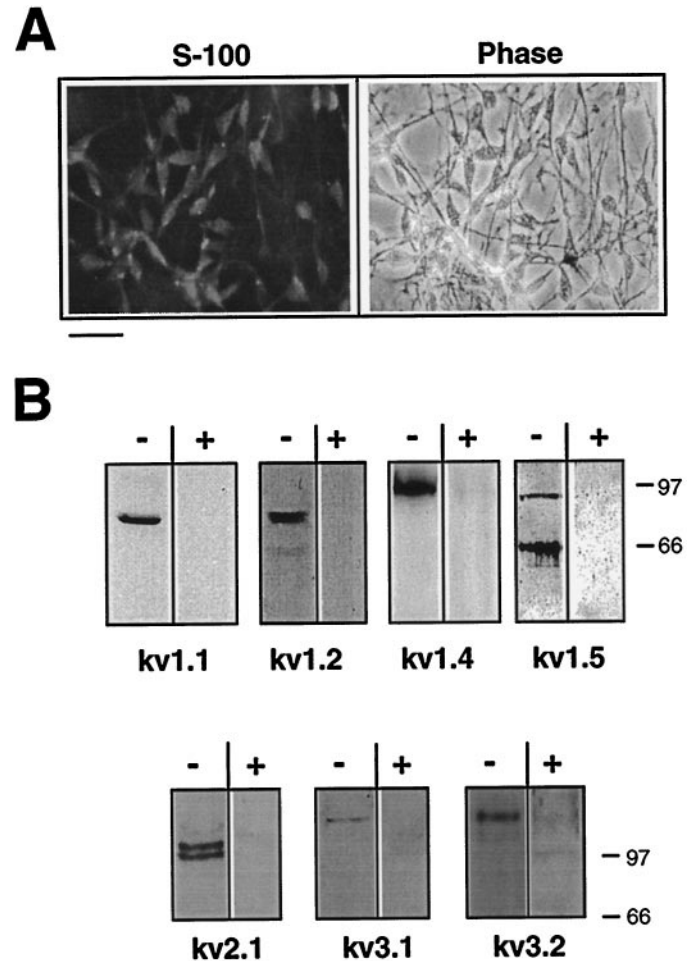
rectly checked by preadsorbing the antisera with their respective antigens (see Materials and Methods; Fig. 3*B*). When possible, we further checked the specificity of staining by using antibodies from two different commercial sources (anti-Kv1.1, Kv1.2, Kv1.4, and Kv1.5 antibodies from Upstate Biotechnology and Alomone Labs) and found an identical labeling pattern (data not shown). In agreement with the molecular cloning data, Figure 3*B* shows that the crude membranal fractions of cultured SCs contained the immunoreactive proteins: Kv1.1 (~75 kDa), Kv1.2 (~85 kDa), Kv1.4 (~115 kDa), Kv1.5 (two bands of 65 and 90 kDa), Kv2.1 (doublet of 105 and 115 kDa), Kv3.1b (~126 kDa), and Kv3.2 (~130 kDa). The RT-PCR cloning did not detect Kv1.3 mRNA, nor did the immunoblot analysis show Kv1.3 immunoreactive protein. A very faint immunostaining was observed for Kv1.6 and Kv2.2 α subunits, suggesting that cultured SCs expressed relatively low levels of these Kv channel proteins (data not shown).
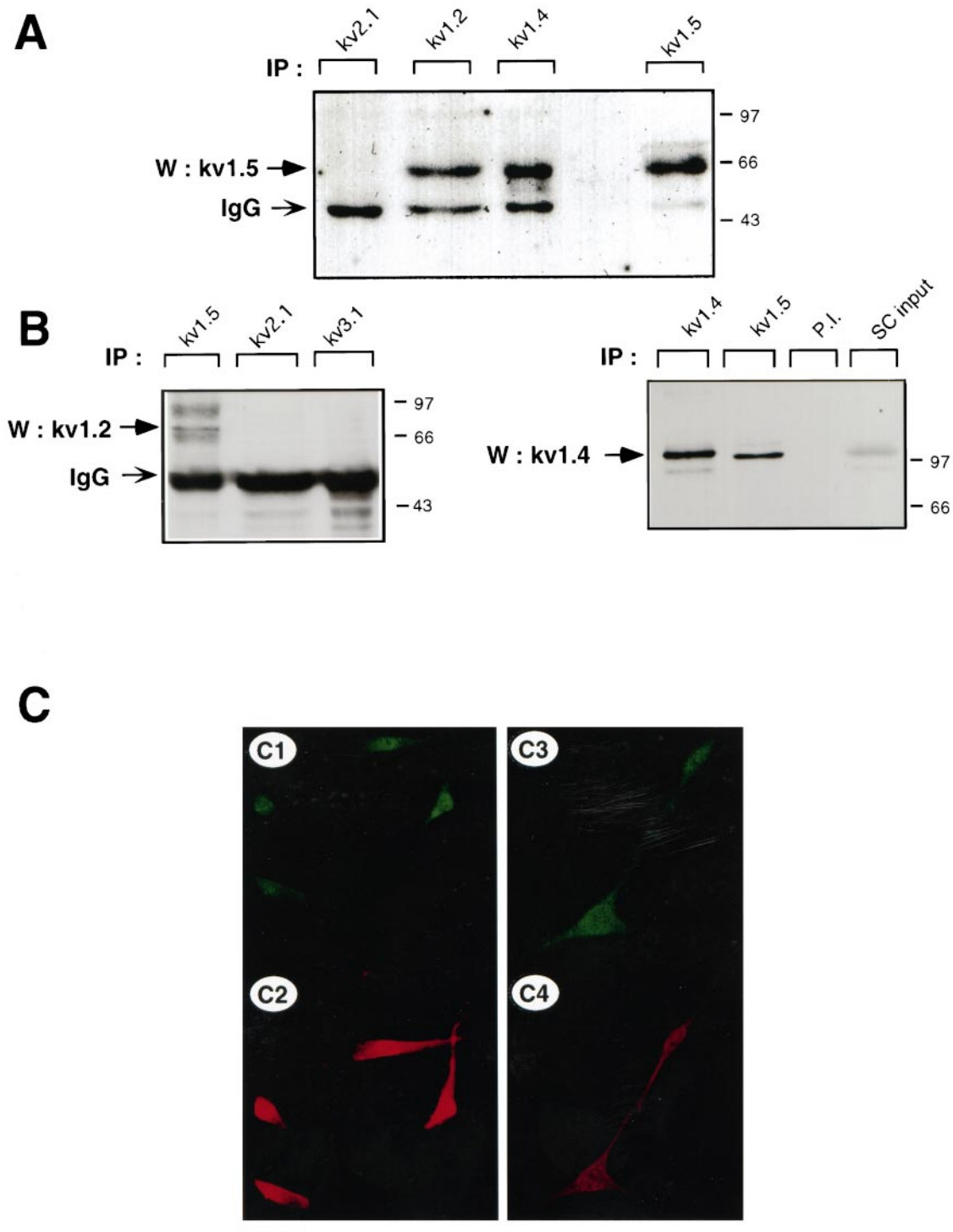
Figure 4. The heteromultimeric association of Kv1.2, Kv1.4, and Kv1.5 α subunits in cultured Schwann cells. *A*, Coimmunoprecipitation of Kv1.5 with other *Shaker*-like subunits. SC membranal fractions were subjected to immunoprecipitation with anti-Kv2.1, anti-Kv1.2, anti-Kv1.4, or anti-Kv1.5 antibodies, and blots were probed with anti-Kv1.5 antibodies. To verify the presence of channel proteins, blots were stripped and reprobed with the respective anti-Kv antibodies (data not shown). Nonspecific bands corresponding to immunoglobulin heavy chain (*IgG*) are also observed. *B*, Reciprocal coimmunoprecipitation of Kv1.2 and Kv1.4 with Kv1.5. *Left*, SC membrane proteins were immunoprecipitated with either Kv1.5, Kv2.1, or Kv3.1 antibodies, and blots were probed with anti-Kv1.2. *Right*, SC membrane proteins were immunoprecipitated with either Kv1.4, Kv1.5, or preimmune antibodies (*P.I.*), and blots were probed with anti-Kv1.4. An aliquot of SC membranes corresponding to ~10% of the proteins used in immunoprecipitation (*SC input*) was used as positive control. *C*, SCs were double labeled with mouse monoclonal anti-Kv1.5 (*C1, C3*) and rabbit polyclonal anti-Kv1.2 (*C2, C4*). Indirect immunofluorescence with anti-mouse FITC and anti-rabbit TRITC was used for detection. Scale bar: *C1–C2*, 35 μM; *C3–C4*, 17 μM.
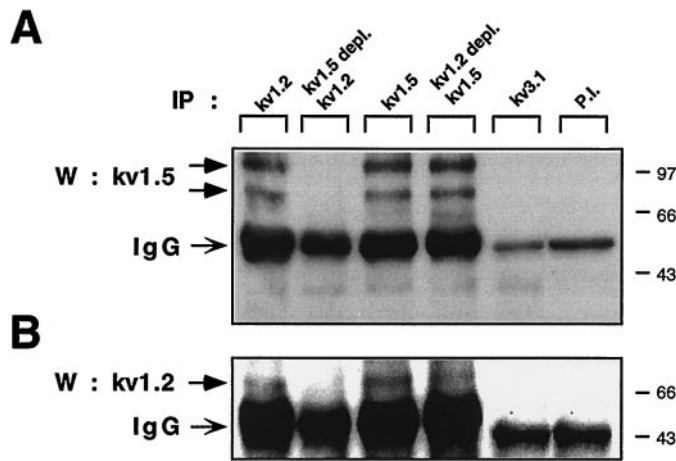
A

Figure 5. The heteromeric association of Kv1.2 and Kv1.5 channel α subunits in sciatic nerve. Reciprocal coimmunoprecipitation of Kv1.5 and Kv1.2 in P4 sciatic nerve is shown. *A*, Homogenates of acutely isolated sciatic nerves from P4 mice were subjected to immunoprecipitation with anti-Kv1.2, anti-Kv1.5, anti-Kv3.1, and preimmune antibodies. The Kv1.2 and Kv1.5 subunits were depleted from sciatic nerve extracts with their respective antibodies, and unbound proteins were subjected to a second round of immunoprecipitation with anti-Kv1.2 (*Kv1.5 depl. Kv1.2*) and anti-Kv1.5 (*Kv1.2 depl. Kv1.5*), respectively. Blots were probed with anti-Kv1.5. *B*, Reciprocal coimmunoprecipitation of Kv1.2 with Kv1.5 in P4 sciatic nerve. The blot shown in *A* was stripped and reprobed with anti-Kv1.2.

Kv1.5, Kv1.2, and Kv1.4 form heteromultimeric complexes in cultured mouse SCs and sciatic nerve

In view of the large and complex molecular repertoire of Kv channel α subunits expressed in SCs, we addressed the question of whether some of the α subunits could be involved in heteromultimeric association. We focused our study on *Shaker* α subunits, because this Kv channel subfamily was the most diversely expressed in SCs. Using a reciprocal immunoprecipitation–immunoblot analysis, we showed that the Kv1.5 α subunits were specifically coimmunoprecipitated from SC membranes by anti-Kv1.2 and anti-Kv1.4 antibodies (Fig. 4*A*). Preimmune antibodies did not precipitate Kv1.5 molecular complexes (Fig. 5). The 65 kDa Kv1.5 protein was the main molecular species to be immunoprecipitated in cultured SCs under these experimental conditions. In contrast to the data obtained with the sciatic nerve (see below; Fig. 5*A*) no detectable 90 kDa species could be observed. As a control, the 65 kDa Kv1.5 subunit could be immunoprecipitated by anti-Kv1.5 antibodies (Fig. 4*A*). No heteromultimeric complexes of Kv1.5 with Kv1.1 could be detected in SCs and sciatic nerve (data not shown). Likewise, neither Kv1.5 nor Kv1.2 formed heteromultimers with Kv channel α subunits from other families (Figs. 4*A*,*B*, 5), such as Kv2.1 (*Shab*) or Kv3.1b (*Shaw*), confirming that only intrafamily Kv channel association can occur (Covarrubias et al., 1991). In reciprocal experiments, we demonstrated that Kv1.2 and Kv1.4 α subunits were coimmunoprecipitated by anti-Kv1.5 but not by anti-Kv2.1 or anti-Kv3.1b antibodies (Figs. 4*B*, 5). Two Kv1.2 broad molecular complexes of ~85 and 95 kDa were specifically precipitated by anti-Kv1.5 antibodies, reflecting a microheterogeneity of Kv1.2 molecules (Fig. 4*B*, *left*). A 115 kDa Kv1.4 molecular species could be precipitated by anti-Kv1.5 antibodies (Fig. 4*B*, *right*). Double-immunofluorescence labeling indicated that Kv1.5 and Kv1.2 were stained rather uniformly on all SC somata and processes, with a slightly sharper staining of Kv1.2 on processes. Overall, the

staining patterns of Kv1.5 and Kv1.2 primarily overlapped in SCs (Fig. 4*C*). These patterns differ from that of Kv2.1, which exhibits membranal clusters around the cell soma (Sobko et al., 1998).

Next, we verified that the occurrence of heteromultimeric complexes of *Shaker* α subunits was not an artifact of culture *in vitro* and could be also found *in vivo* in the sciatic nerve from P4 mice. Figure 5 shows that, as in cultured SCs, Kv1.5 and Kv1.2 could be specifically and reciprocally coimmunoprecipitated from the sciatic nerve *in vivo*. The 65 kDa Kv1.5 species was very weakly immunoprecipitated. Rather, the 90 kDa and a higher molecular weight species of ~110 kDa were the primary Kv1.5 molecular complexes immunoprecipitated by both anti-Kv1.5 and anti-Kv1.2 antibodies. This might reflect differential posttranslational processing of Kv1.5 in P4 sciatic nerve compared with other postnatal stages (see below; Fig. 6) and SCs in culture. Using sequential rounds of immunoprecipitation (Shamotienko et al., 1997), we depleted Kv1.5 α subunits from the P4 sciatic nerve extracts with anti-Kv1.5 antibodies. This depletion totally prevented the subsequent immunoprecipitation of Kv1.5 with anti-Kv1.2 antibodies, thus demonstrating the specificity of the precipitation protocol (Fig. 5). When Kv1.2 α subunits were depleted from the nerve extracts with anti-Kv1.2 antibodies, a substantial fraction of Kv1.5 protein could still be subsequently immunoprecipitated with anti-Kv1.5 antibodies, indicating that the pool of Kv1.5 α subunits is not involved exclusively in heteromultimeric association with Kv1.2 subunits. Interestingly, when Kv1.5 α subunits were depleted from the P4 sciatic nerve extracts with anti-Kv1.5 antibodies, no Kv1.2 subunit could subsequently be immunoprecipitated by anti-Kv1.2 antibodies, suggesting that most of the Kv1.2 α subunits are involved in heteromultimeric association with Kv1.5 subunits.

Developmental profile of Kv channel α subunits in the postnatal sciatic nerve

Physiological studies have shown that K_D and K_{IR} channels are downregulated in the soma as myelination proceeds and proliferation ceases (Konishi, 1990; Wilson and Chiu, 1990a). Because of the diversity of Kv channel proteins, which could contribute to K_D channel activity, it was important to analyze the developmental profile of the various Kv channel α subunits in the developing sciatic nerve. Semiquantitative RT-PCR showed that there was a significant (42 ± 9 and $68 \pm 7\%$) downregulation ($n = 4$; $p < 0.01$) of Kv1.5 and Kv1.2 mRNAs, respectively, in the mouse sciatic nerve from P1 to P40 (Fig. 6*A*,*B*, *right panels*). Similarly, Western blot analysis indicated that there was a 38 ± 8 and $68 \pm 8\%$ downregulation ($n = 3$; $p < 0.05$) of the Kv1.5 and Kv1.2 immunoreactive proteins, respectively, from P1 to P40 (Fig. 6*A*,*B*,*C*). Interestingly, the 90 kDa Kv1.5 species was expressed exclusively at P4 and subsequently disappeared at later developmental stages. Immunoblot data indicated that there was also an abrupt drop in Kv1.2 of >70% from P8 to P40 ($n = 3$). Likewise, there was a marked decrease in Kv2.1 ($47 \pm 6\%$; $n = 3$) and Kv3.1b ($64 \pm 10\%$; $n = 3$) immunoreactive proteins from P4 to P40, with an early downregulation at P8 for Kv3.1b (Fig. 7). A contrasting pattern was obtained with the Kv1.4 immunoreactive protein, whose levels did not change substantially throughout the postnatal period (Fig. 7). In addition to the 115 kDa species found in cultured SCs, a 94 kDa Kv1.4 immunoreactive protein was also specifically detected at all postnatal stages in the sciatic nerve.
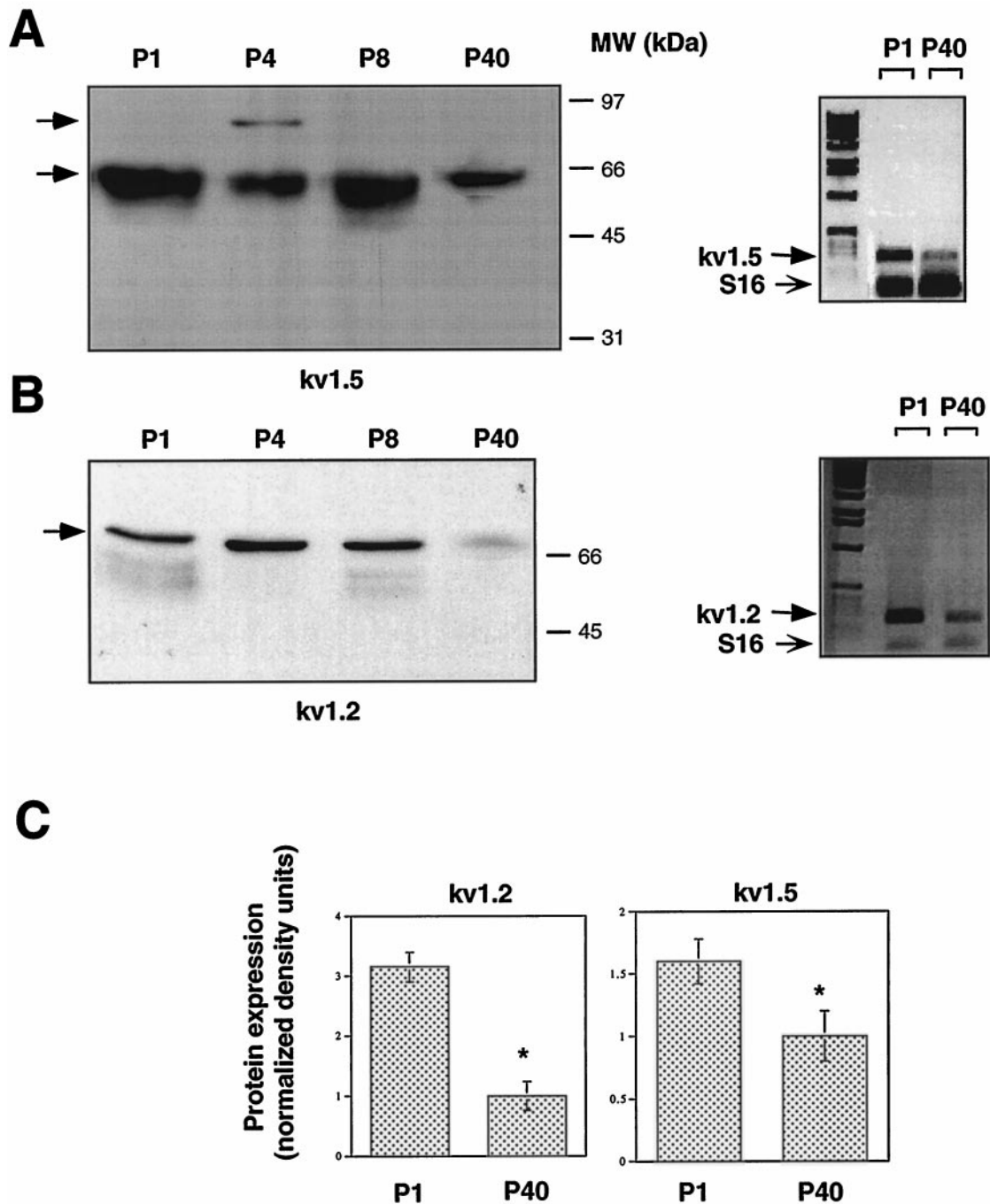
Figure 6. Expression of Kv1.2 and Kv1.5 channel α subunits in mouse sciatic nerve during postnatal development. *A, Left*, Membrane fractions of sciatic nerves from P1, P4, P8, and P40 mice were subjected to SDS-PAGE and immunoblot analysis with anti-Kv1.5 antibodies. To estimate and compare total protein inputs in each lane, blots were stained with Ponceau S before immunoblot analysis (data not shown). *Right*, RT-PCR, followed by Southern blot analysis of Kv1.5 transcripts in sciatic nerves from P1 and P40 mice. *B, Left*, Immunoblot analysis of Kv1.2 on postnatal sciatic nerve as in *A*. *Right*, RT-PCR and Southern blot analysis of Kv1.2 as in *A*. Primer pairs to the specific 3′ coding regions of either Kv1.5 (*A*) or Kv1.2 (*B*) amplified PCR fragments of 273 and 248 bp, respectively. The *bottom band* represents the S16 ribosomal protein PCR fragment (102 bp), which was used to estimate the starting input RNA. *C*, Quantitation of the developmental downregulation of Kv1.2 and Kv1.5 proteins from P1 to P40 sciatic nerve as illustrated in *A* and *B*. Data of densitometric scanning were normalized to values of P40 and represent mean $\pm$ SEM of three independent experiments. *$p < 0.05$, differs significantly from P40.

Proliferation of mouse SCs is blocked by broad-spectrum K$^+$ channel blockers but not by specific Kv1.1, Kv1.2, Kv1.3, and Kv1.6 channel toxin blockers

To compare the ability of various K$^+$ channel blockers to depress the SC K$^+$ currents with their capacity to inhibit SC proliferation,

we measured [^{3}H]thymidine incorporation in proliferating SCs in the absence and presence of broad-spectrum K$^+$ channel blockers, as well as more selective channel toxins. SCs grown in the presence of 10% FCS exhibited a high level of [^{3}H]thymidine incorporation (Fig. 8*A*). Serum deprivation (DMEM–F-12) in-
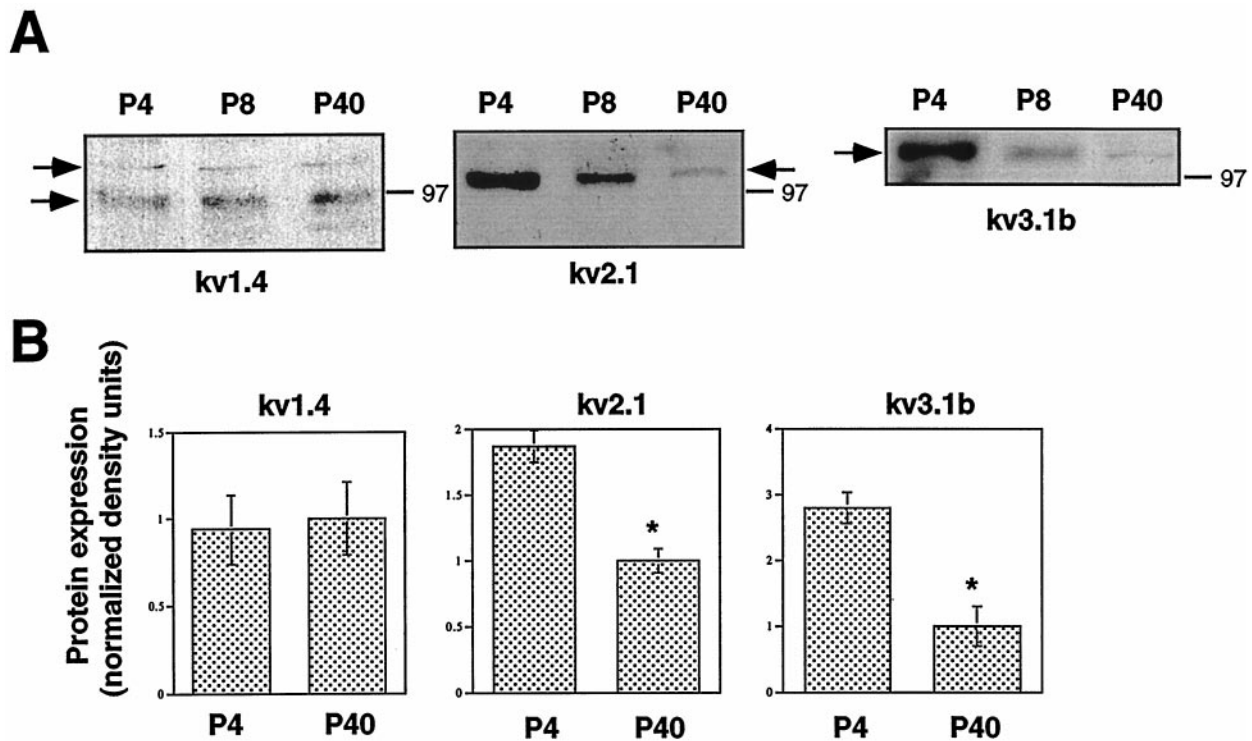
Figure 7. Postnatal developmental profile of Kv1.4, Kv2.1, and Kv3.1b in the sciatic nerve. *A*, Immunoblot analysis of sciatic nerve membranal extracts from P4, P8, and P40 mice with anti-Kv1.4, anti-Kv2.1, and anti-Kv3.1b antibodies. *B*, Quantitation of the developmental changes were performed as described in Figure 6. Data of densitometric scanning were normalized to values of P40 and represent mean ± SEM of three independent experiments. *$p < 0.05$, differs significantly from P40.

hibited SC proliferation by >80%. SCs grown in serum-free defined medium, such as SATO1 (medium containing insulin and transferrin), had substantial proliferative capacity, reaching a level of ~60% of that obtained in the presence of 10% serum. Interestingly, when growth factors, such as PDGF (5 ng/ml) and bFGF (5 ng/ml), were added to the defined medium (SATO2), SC proliferation was further enhanced, reaching values ~85% of that found with 10% serum (Fig. 8*A*).

SC proliferation, measured in the presence of 10% serum, was generally sensitive to blockade by broad-spectrum K$^+$ channel blockers, such as 10 mM TEA, 0.5 mM Ba^{2+}, 100 μM quinine, 3 mM 4-AP, 100 μM quinidine, and 10 μM clofilium with 48, 45, 98, 57, 87, and 74% block, respectively ($n = 4$) (Fig. 8*B*). In contrast, K$^+$ channel toxins, such as CTX (10 nM), DTX (10 nM), and AgTx (10 nM), did not affect SC proliferation ($n = 4$) (Fig. 8*B*). Similar results were obtained when the channel toxin concentration was raised to 100 nM (data not shown).

DISCUSSION

In the neonatal and early postnatal periods (P1–P8), mouse SCs are known to express K_{IR}, K_A, and K_D channel activities (Konishi, 1990; Amedee et al., 1991; Verkhartsky et al., 1991a,b). A direct comparison of the biophysical and pharmacological properties of native currents with those of cloned channels expressed in heterologous systems is always difficult, often because of overlapping characteristics of Kv channel α subunits, heteromultimeric association, interaction with β subunits, and cell-specific posttranslational modifications (e.g., phosphorylation). Recent studies have begun to address the molecular identity of K$^+$ channels in SCs. It was found that the *Shaker*-like delayed-rectifier Kv1.1, Kv1.2, and Kv1.5 and the inward-rectifier IRK1

and IRK3 α subunits are expressed in SCs of the rat sciatic nerve (Chiu et al., 1994; Mi et al., 1995, 1996; Rasband et al., 1998). The present work confirms and extends these previous studies. Interestingly, we have isolated cDNAs and identified proteins, such as Kv2.1, Kv3.1b, and Kv3.2, which belong to *Shab*- and *Shaw*-families of noninactivating K$^+$ channel α subunits. This finding suggests that the predominant K_D current expressed in SCs is not exclusively encoded by *Shaker*-like α subunits but could be also accounted for by the activity of *Shab*-related (Kv2.1) and *Shaw*-related (Kv3.1b, Kv3.2) channel complexes. As for the K_A current, we show here that the Kv1.4 subunit is expressed in SCs and sciatic nerve. In the molecular screening process, we were unable to identify any other inactivating Kv channel α subunits, such as Kv1.3, Kv3.4, or Kv4.2. Although we cannot exclude the presence of such subunits in SCs, these experiments indicate that K_A current is accounted for by the activity of a channel complex comprising Kv1.4 α subunits, either as homomultimers or/and heteromultimers. Importantly, we found that Kv1.4 could form heteromultimers with Kv1.5 subunits; such heteromultimers may generate an inactivating K$^+$ current. Indeed, when expressed in *Xenopus* oocytes in a 1:1 ratio, heteromultimers of Kv1.5 and Kv1.4 were found to generate a transient K$^+$ current with inactivation time constants (τ, ~40 msec) similar to those found in SCs (Po et al., 1993). Inactivation of K_A current could also be regulated by the presence of β subunits in the channel complex. Although a recent study showed that the β2 subunits are not expressed in rat SCs (Rasband et al., 1998), the status of other β subunits in SCs remains to be examined.

Kv1.2 transcripts were detected previously in SCs; however, protein expression has not been documented so far (Chiu et al.,
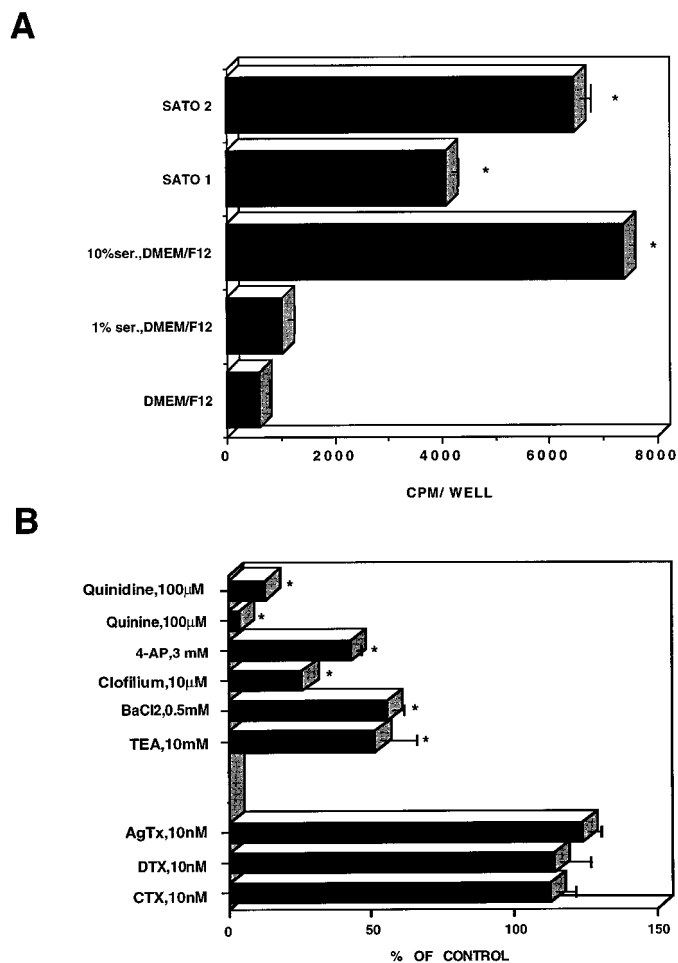
A

B

Figure 8. Effect of Kv channel blockers on Schwann cell proliferation. *A*, [^{3}H]Thymidine incorporation (0.2 μCi/well) was assayed in SCs cultured as indicated, in serum-containing medium, in serum-deprived medium (DMEM–F-12), or in serum-free defined medium supplemented with either 5 μg/ml insulin, 5 μg/ml transferrin, and 5 ng/ml sodium selenite (*SATO1*) or with SATO1 containing 5 ng/ml PDGF and 5 ng/ml bFGF (*SATO2*). *B*, Proliferation was assayed in cultured SCs exposed for 24 hr to various channel blockers at the indicated concentrations in the presence of 10% FCS. The results were expressed as percentage of maximal serum-stimulated proliferation. Data points represent the mean ± SEM of four independent experiments, each performed in triplicate.

1994; Mi et al., 1995; Rasband et al., 1998). Using the reciprocal coimmunoprecipitation strategy, we show here that the Kv1.5 subunits could form heteromultimeric complexes with Kv1.4 and Kv1.2 in both cultured SCs and sciatic nerve. Furthermore, immunodepletion–immunoprecipitation experiments performed in the P4 sciatic nerve indicate that most of the Kv1.2 channel subunits seem to be involved in heteromultimeric association with Kv1.5, whereas the pool of Kv1.5 α subunits is not exclusively involved in heteromultimeric association with Kv1.2 subunits. Obviously, this feature found in the P4 sciatic nerve may not apply entirely for cultured SCs *in vitro*. Although Kv1.2 clearly forms heteromultimers with Kv1.5 in both cultured SCs and the sciatic nerve, the ratio of Kv1.2/Kv1.5 heteromultimers over the total pool of Kv1.2 may be different in cultured SCs compared with the P4 sciatic nerve. The immunostaining pattern of Kv1.5 and Kv1.2 seems to overlap in cultured SCs; however, resolutive confocal studies, especially in the sciatic nerve, are clearly needed to address the colocalization issue. Interestingly, although Kv1.1

is expressed in both SCs and sciatic nerve, we could not detect heteromultimeric complexes of Kv1.5 with Kv1.1. Our findings are in line with previous studies showing a differential subcellular immunolocalization of Kv1.1 and Kv1.5 proteins, thus providing evidence against their heteromultimeric coassembly (Mi et al., 1995; Rasband et al., 1998).

DTX blocks homomultimeric Kv1.1, Kv1.2, and Kv1.6 channels with high affinity (Grissmer et al., 1994). This feature implies that there are very few, if any, homomultimeric DTX-sensitive Kv1.1 and Kv1.2 functional channel complexes in SCs. Despite the rather abundant expression of Kv1.2 subunits in mouse SCs, the insensitivity of K$^+$ currents to DTX suggests at least two possible explanations. First, assuming that native Kv1.2/Kv1.5 heteromultimeric channels are DTX-sensitive, then one should consider that this channel complex has a minor contribution to SC K_D currents. For example, the Kv1.2/Kv1.5 channels may not be functional. In this regard, we showed that Kv2.1 and Kv3.1 are also expressed in SCs and probably account for a substantial part of K_D currents (Sobko et al., 1998; present study). Second, assuming that the coassembly of Kv1.2 with the DTX-insensitive Kv1.5 subunit results in DTX-insensitive channels, then the SC K_D currents would be accounted for by the concerted activity of essentially DTX-insensitive channel complexes of the Kv1, Kv2, and Kv3 families. In support of this explanation, previous studies showed that the association rate of α DTX depends on the number of DTX-sensitive α subunits in a channel complex, suggesting that all four DTX-sensitive α subunits must interact with the toxin to produce a high-affinity binding site (Tytgat et al., 1995). A similar mechanism of additive contributions has been also characterized for TEA on *Shaker*-type channels (Heginbotham and MacKinnon, 1992; Liman et al., 1992). However, other studies showed that the heteromultimeric assembly of Kv1.2 with the DTX-insensitive Kv1.4 subunit does not follow an additivity model but rather a single subunit model by conferring the DTX sensitivity of the channel complex (Ruppersberg et al., 1990; Hopkins, 1998). In our hands, equimolar expression of Kv1.2 and Kv1.5 subunits in *Xenopus* oocytes results in K$^+$ currents that are insensitive to 30 nm DTX (B. Attali and A. Peretz, unpublished data). The nature of the toxin-insensitive subunit is probably a crucial determinant of the heteromultimeric channel behavior. For example, Russel et al. (1994) showed that the assembly of the CTX-sensitive Kv1.2 subunit with Kv1.5 surprisingly results in a CTX-insensitive channel complex that follows a dominant negative behavior rather than a single subunit model (MacKinnon, 1991). This feature is in line with our data, because the mouse SC K$^+$ currents were insensitive to CTX (100 nm). Furthermore, we did not detect any Kv1.3 mRNA or protein in SCs and sciatic nerve. Regarding the pharmacology of the broad-spectrum K$^+$ channel blockers, with few exceptions, most of the Kv channel α subunits we identified display relatively high affinities for TEA and 4-AP (Pongs, 1992).

It has been suggested that in rodent SCs K$^+$ channels play a role in buffering activity-dependent K$^+$ accumulation during early myelinogenesis via a spatial buffering mechanism or via K$^+$ siphoning (Konishi, 1990; Chiu, 1991). The localization found previously for Kv1.5 in the outer SC membrane near the node indicates that it is not ideally suited for this function (Mi et al., 1995). The inward-rectifier K$^+$ channels IRK1 and IRK3 found in the nodes on SC microvilli were proposed as better candidates for K$^+$ buffering activity (Mi et al., 1996). The other important function proposed for SC K$^+$ channels is their role in SC proliferation. K_D channels are thought to be linked to SC proliferation

during development and after Wallerian degeneration of sciatic nerves (Chiu and Wilson, 1989; Konishi, 1989; Wilson and Chiu, 1990a). Mitogenic factors, such as axon and myelin fragments or glial growth factor, were shown to increase K_D channel activity and rat SC proliferation (Wilson and Chiu, 1993). More recently, we found that K_D channels are constitutively activated by a Src family tyrosine kinase in SCs, further suggesting their role in SC proliferation (Sobko et al., 1998). In the present work, we show that there is a substantial correlation between the responsiveness of the K$^+$ currents and SC proliferation to particular channel blockers. Whereas the broad-spectrum K$^+$ channel blockers were efficient, with quinidine, quinine, clofilium, and 4-AP being the most potent, the more selective channel toxins were totally ineffective on both assays, in agreement with the biochemical data.

Physiological studies performed on freshly dissociated SCs of the developing sciatic nerve showed that a noninactivating outward K$^+$ current is downregulated during SC development and differentiation (Wilson and Chiu, 1990a; Konishi, 1990). This decrease in K_D current expression has been linked to the diminished ability of SCs to proliferate as differentiation proceeds and myelination begins (Wilson and Chiu, 1990a; Konishi, 1990). The present data are consistent with these developmental studies. We show that all Kv channel α subunits expressed in the sciatic nerve and encoding noninactivating delayed-rectifier K$^+$ channels are markedly downregulated from P1 to P40. These include Kv1.2, Kv1.5, Kv2.1, and Kv3.1b. The unique exception to this developmental profile is Kv1.4, whose expression remains approximately constant during the same postnatal period. This pattern of development at the protein level contrasts with that found for most Kv channel α subunits expressed in the developing brain in which there is a progressive upregulation from early to late postnatal stages (Maletic-Savatic et al., 1995). It is worth noting that the 90 kDa species for Kv1.5 was observed primarily at P4, whereas the 65 kDa isoform was detected throughout postnatal developmental periods. Although the significance of this 90 kDa species is unclear, it may reflect a Kv1.5 posttranslational modification specific to a premyelinating stage of SCs. This 90 kDa isoform is consistently observed also in cultured SCs (Sobko et al., 1998; present study). Our data are similar to those of Chiu et al. (1994), showing a decrease in Kv1.1 and Kv1.2 mRNA levels in the rat sciatic nerve from P15 to P90. In the developmental analysis presented in this work, the relative contributions of Kv channels originating from SCs and those belonging to axonal membranes are not known. With respect to Kv1.5, its contribution essentially originates from SCs, because no expression was found in sciatic axonal membranes (Mi et al., 1995). For the other subunits, we found a similar downregulation pattern at the mRNA level, indicating that the transcripts and the proteins primarily originate from SCs. However, a substantial source of Kv channel protein could belong to axonal membranes (e.g., Kv1.2; see Rasband et al., 1998). In future studies, it will be important to determine the subcellular localization of this complex repertoire of Kv channel α subunits along the sciatic nerve.

In summary, this study indicates that a diverse and complex repertoire of Kv channel α subunits is expressed in cultured mouse SCs and sciatic nerve. We have detected heteromultimeric channel complexes consisting of either Kv1.5 and Kv1.2 or Kv1.5 and Kv1.4. In P4 sciatic nerve, most of the Kv1.2 channel subunits appear to be involved in heteromultimeric association with Kv1.5. We also showed that all Kv channel α subunits encoding K_D channel activity are markedly downregulated in the developing sciatic nerve, reaching lowest levels of protein expression at P40.

Our results suggest that in SCs developmentally regulated patterns of defined K$^+$ channel complexes underlie K_D currents and confirm that K_D channels are important for SC proliferation.

REFERENCES

Amedee T, Ellie E, Dupouy B, Vincent JD (1991) Voltage-dependent calcium and potassium channels in Schwann cells cultured from dorsal root ganglia of the mouse. J Physiol (Lond) 441:35–56.

Attali B, Lesage F, Ziliani P, Guillemare E, Honore E, Waldman R, Hugnot JP, Mattei MG, Lazdunski M, Berhanin J (1993) Multiple mRNA isoforms encoding the mouse cardiac Kv1–5 delayed rectifier K$^+$ channel. J Biol Chem 268:24283–24289.

Attali B, Wang N, Kolot A, Sobko A, Cherepanova V, Soliven B (1997) Characterization of delayed rectifier Kv channels in oligodendrocytes and progenitor cells. J Neurosci 17:8234–8245.

Baker MD, Ritchie JM (1993) Two types of 4-aminopyridine-sensitive potassium current in rabbit Schwann cells. J Physiol (Lond) 464:321–342.

Barres BA, Chun LLY, Corey DP (1990) Ion channels in vertebrate glia. Annu Rev Neurosci 13:441–474.

Brockes JP, Fields KL, Raff MC (1979) Studies on cultured rat Schwann cells. I. Establishment of purified populations from cultures of peripheral nerve. Brain Res 165:105–118.

Chiu SY (1991) Functions and distribution of voltage-gated sodium and potassium channels in mammalian Schwann cells. Glia 4:541–558.

Chiu SY, Wilson GF (1989) The role of potassium channels in Schwann cell proliferation in Wallerian degeneration of explant rabbit sciatic nerve. J Physiol (Lond) 408:199–222.

Chiu SY, Shrager P, Ritchie JM (1984) Neuronal type Na$^+$ and K$^+$ channels in rabbit cultured Schwann cells. Nature 311:156–157.

Chiu SY, Scherer SS, Blonski M, Kang SS, Messing A (1994) Axons regulate the expression of Shaker-like potassium channel genes in Schwann cells in peripheral nerve. Glia 12:1–11.

Covarrubias M, Wei AA, Salkoff L (1991) Shaker, Shal, Shab, and Shaw express independent K$^+$ current systems. Neuron 7:763–773.

Garcia ML, Garcia-Calvo M, Hidalgo P, Lee A, MacKinnon R (1994) Purification and characterization of three inhibitors of voltage-dependent K$^+$ channels from *Leiurus quinquestriatus* var. hebraeus venom. Biochemistry 33:6834–6839.

Grissmer S, Nguyen AN, Aiyar J, Hanson DC, Mather RJ, Gutman GA, Karmilowicz MJ, Auperin DD, Chandy KG (1994) Pharmacological characterization of five cloned voltage-gated K$^+$ channels, types Kv1.1, 1.2, 1.3, 1.5, and 3.1, stably expressed in mammalian cell lines. Mol Pharmacol 45:1227–1234.

Hamill OP, Marty A, Neher E, Sakmann B, Sigworth FJ (1981) Improved patch-clamp techniques for high-resolution current recording from cells and cell-free membrane patches. Pflügers Arch 391:85–100.

Heginbotham L, MacKinnon R (1992) The aromatic binding site for tetraethyl ammonium ion on potassium channels. Neuron 8:483–491.

Hopkins WF (1998) Toxin and subunit specificity of blocking affinity of three peptide toxins for heteromultimeric voltage-gated potassium channels expressed in *Xenopus* oocytes. J Pharmacol Exp Ther 285:1051–1060.

Hoppe D, Lux H-D, Schachner M, Kettenman H (1989) Activation of K$^+$ currents in cultured Schwann cells is controlled by extracelllular pH. Pflügers Arch 415:22–28.

Konishi T (1989) Voltage-dependent potassium channels in mouse Schwann cells. J Physiol (Lond) 411:115–130.

Konishi T (1990) Voltage-gated potassium currents in myelinating Schwann cells in the mouse. J Physiol (Lond) 431:123–139.

Laemmli EK (1970) Cleavage of structural proteins during the assembly of the head of bacteriophage T4. Nature 227:680–685.

Liman ER, Tytgat J, Hess P (1992) Subunit stoichiometry of a mammalian K$^+$ channel determined by construction of multimeric cDNAs. Neuron 9:861–871.

MacKinnon R (1991) Determination of the subunit stoichiometry of a voltage-activated potassium channel. Nature 350:232–235.

Maletic-Savatic M, Lenn NJ, Trimmer JS (1995) Differential spatiotemporal expression of K$^+$ channel polypeptides in rat hippocampal neurons developing *in situ* and *in vitro*. J Neurosci 15:3840–3851.

Mi H, Deerink TJ, Ellisman MH, Schwarz TL (1995) Differential distribution of closely related potassium channels in rat Schwann cells. J Neurosci 15:3761–3774.

Mi H, Deerink TJ, Jones M, Ellisman MH, Schwarz TL (1996) Inwardly

rectifying K$^+$ channels that may participate in K$^+$ buffering are localized in microvilli of Schwann cells. J Neurosci 16:2421–2429.

Mirsky R, Jessen KR (1996) Schwann cell development, differentiation and myelination. Cur Opin Neurobiol 6:89–96.

Po S, Roberds S, Snyders DJ, Tamkun MM, Bennet PB (1993) Heteromultimeric assembly of human potassium channels. Circ Res 72:1326–1336.

Pongs O (1992) Molecular biology of voltage-dependent potassium channels. Physiol Rev 72:S69–S88.

Rasband MN, Trimmer JS, Schwarz TL, Levinson SR, Ellisman MH, Schachner M, Shrager P (1998) Potassium channel distribution, clustering, and function in remyelinating rat axons. J Neurosci 18:36–47.

Ritchie JM (1992) Voltage-gated ion channels in Schwann cells and glia. Trends Neurosci 15:345–351.

Ruppersberg JP, Schroter KH, Sakmann B, Stocker M, Sewing S, Pongs O (1990) Heteromultimeric channels formed by rat brain potassium-channel proteins. Nature 345:535–537.

Russell SN, Overturf KE, Horowitz B (1994) Heterotetramer formation and charybdotoxin sensitivity of two K$^+$ channels cloned from smooth muscle. Am J Physiol 267:C1729–C1733.

Shamotienko OG, Parcej DN, Dolly JO (1997) Subunit combinations defined for K$^+$ channel Kv1 subtypes in synaptic membranes from bovine brain. Biochemistry 36:8195–8201.

Shrager P, Chiu SY, Ritchie JM (1985) Voltage-dependent sodium and potassium channels in mammalian cultured Schwann cells. Proc Natl Acad Sci USA 82:948–952.

Sobko A, Peretz A, Attali B (1998) Constitutive activation of voltage-gated K$^+$ channels by Src-family protein tyrosine kinase in Schwann cells. EMBO J 17:4723–4734.

Sontheimer H (1994) Voltage-dependent ion channels in glial cells. Glia 11:156–172.

Tytgat J, Debont T, Carmeliet E, Daenens P (1995) The α-dendrotoxin footprint on a mammalian potassium channel. J Biol Chem 270:24776–24781.

Verkhartsky A, Hoppe D, Kettenman H (1991a) Single K$^+$ channel properties in cultured mouse Schwann cells: conductance and kinetics. J Neurosci Res 28:200–209.

Verkhartsky A, Hoppe D, Kettenman H (1991b) K$^+$ channel properties in cultured mouse Schwann cells: dependence on extracellular K$^+$. J Neurosci Res 28:210–216.

Wang Z, Fermini B, Nattel S (1995) Effects of flecainide, quinidine, and 4-aminopyridine on transient outward and ultrarapid delayed rectifier currents in human atrial myocytes. J Pharmacol Exp Ther 272:184–196.

Wilson GF, Chiu SY (1990a) Potassium channel regulation in Schwann cells during early developmental myelinogenesis. J Neurosci 10:1615–1625.

Wilson GF, Chiu SY (1990b) Ion channels in axon and Schwann cell membranes at paranodes of mammalian myelinated fibers studied with patch clamp. J Neurosci 10:3263–3274.

Wilson GF, Chiu SY (1993) Mitogenic factors regulate ionic channels in Schwann cells cultured from newborn rat sciatic nerve. J Physiol (Lond) 470:501–520.

Yeh JZ, Oxford GS, Wu CH, Narahashi T (1976) Dynamics of aminopyridine block of potassium channels in squid axon membrane. J Gen Physiol 68:519–535.

Zorick TS, Lemke G (1996) Schwann cell differentiation. Curr Opin Cell Biol 8:870–876.